PHYSICAL REVIEW B VOLUME 61, NUMBER 21 1 JUNE 2000-I

Order-disorder transition in hcp binary alloys: Next-nearest-neighbor interactions

Masato Shimono and Hidehiro Onodera
National Research Institute for Metals, 305-0047 Tsukuba, Japan

(Received 2 March 2000)

The order-disorder transition in hcp binary alloys is investigated by Monte Carlo simulations and the renormalization-group methods. The inclusion of the interactions beyond the nearest neighbors induces qualitative changes of the phase boundaries. Especially, the contribution from second-neighbor interactions explains the shift along the concentration axis of the congruent point of order-disorder transition observed in the α/α_2 phase boundaries in the Ti-Al binary system.

The phase structure of the Ising model equivalent to binary alloy systems has been studied by both numerical and analytic methods such as Monte Carlo simulations,[1–8] cluster variation methods (CVM),[9–15] and renormalization-group calculations.[16–19] However, most of these studies have focused on cubic structures such as fcc and bcc lattices, and a little has been investigated on hcp lattices.[20–26] Especially, the experimentally observed order-disorder phase boundaries in hcp Ti-Al alloys show[27] a considerable shift to the higher Al concentration from the stoichiometry, which can never be understood within the framework of nearest-neighbor pair interactions.[26] In this work we investigate the effect of the interactions beyond the nearest neighbors on the order-disorder transition in hcp binary alloys by using Monte Carlo simulations and the renormalization-group methods.

We first define the ith neighbors in hcp lattices as illustrated in Fig. 1. Among the nearest neighbors we distinguish the neighbors within a basal plane from the neighbors between adjacent planes in order to take the tetragonality into account. Here we suppose the binary $A_{1-x}B_x$ system interacting with the pairwise energies E^i_{AB} between the ith neighbor pair of elements A and B. If we define the interaction parameter W_i as

$$W_i = E^i_{AB} - \frac{1}{2}(E^i_{AA} + E^i_{BB}), \tag{1}$$

the total Hamiltonian of the system can be written by

$$H = \sum_i W_i N^i_{AB} + \mu_A N_A + \mu_B N_B, \tag{2}$$

where N^i_{AB} is the number of ith neighbor AB pairs, N_A and N_B are the numbers of each element, and μ_A and μ_B are the effective chemical potentials of the pure elements. If we introduce the parameter $\xi_i = W_i/W_0$, the system can be uniquely determined by W_0, ξ_1, ξ_2, and ξ_3. Especially, the deviation of ξ_1 from unity corresponds to the anisotropy of the axial ratio c/a.

Since we are mainly interested in D0$_{19}$ ordered structure observed as the α_2 phase in the Ti-Al binary system, we shall confine ourselves in the system with antiferromagnetic nearest-neighbor interactions and ferromagnetic next-nearest-neighbor interactions in this study. That corresponds to the parameter region $W_0 < 0$, $\xi_1 \sim 1$, and $\xi_2, \xi_3 \leqslant 0$, where D0$_{19}$ (A_3B) and B19 (AB) ordered phases and A3 disordered phase are dominant phases at high temperatures.

In the Monte Carlo simulations, we have mainly used a hcp lattice of $24\times24\times32 = 18432$ sites with periodic boundary conditions. A smaller system ($12\times12\times16$) and a larger system ($48\times48\times64$) have been also used to check the finite-size effect in some cases, and it proved not to change the results so much. The calculations have been performed on the grand canonical ensemble in which the independent variables are chemical potential difference $\mu = \mu_A - \mu_B$ and the temperature T. The phase boundaries has been determined by the following procedure.[3,6,24] By thermal equilibration of the system with various parameter sets (μ, T), we first obtain the phase diagram on the μ-T plane, next we examine the relation between μ and the composition x in each phase, then we can calculate the phase diagram on the x-T plane.

Figure 2 shows the calculated phase diagram for $\xi_1 = 1.0$ and $\xi_2 = \xi_3 = 0.0$. It corresponds to the hcp or fcc lattices with isotropic nearest-neighbor interactions and well coincides with those found in the literatures.[6,8,24] Here we have defined the reduced temperature normalized by the average coupling $(W_0 + W_1)/2$, which corresponds to the formation energy of D0$_{19}$ phase. We note that the composition of the congruent point of D0$_{19}$/A3 transition already deviates a little to the higher concentration from the stoichiometric value 0.25 even in the isotropic case.

Figure 3 shows the effect of tetragonality. That is, it shows the phase boundaries with the variations of ξ_1 from 0.9 to 1.1 under keeping $\xi_2 = \xi_3 = 0.0$. In order to concentrate on the order-disorder phase boundaries around $x = 0.25$, only D0$_{19}$/A3 phase boundaries are depicted. The effect of variation of anisotropy ratio on the shape of the phase boundaries is rather weak and the composition of the congruent point

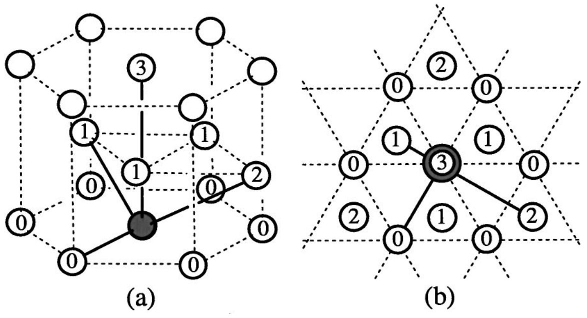

FIG. 1. Perspective view (a) and top view (b) of the hcp lattice. The ith neighbors to the central atom (shaded) are denoted by the encircled number i.

0163-1829/2000/61(21)/14271(4)/$15.00

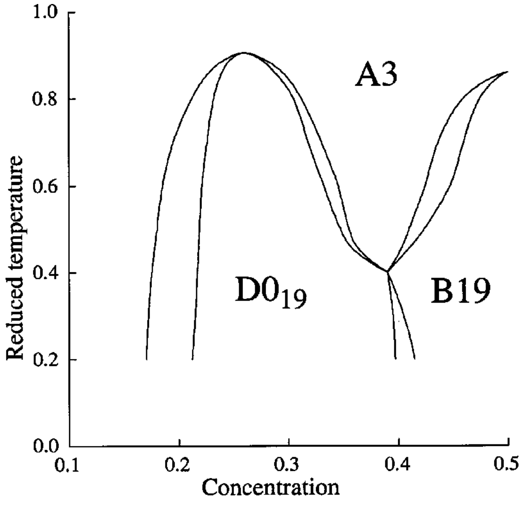

FIG. 2. Calculated phase diagram for $\xi_1 = 1.0$ and $\xi_2 = \xi_3 = 0.0$. Reduced temperature is defined as $2kT/(W_0 + W_1)$.

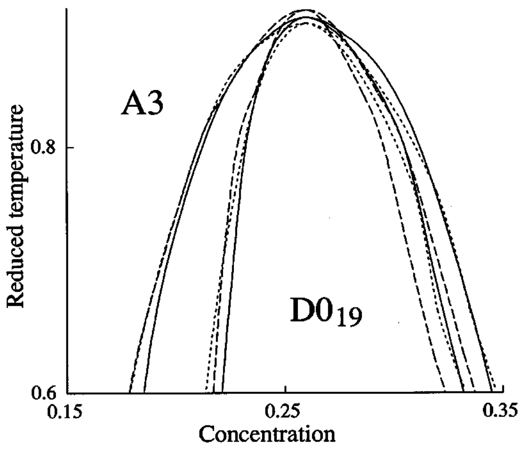

FIG. 3. Changes of the $D0_{19}/A3$ phase boundaries with the variations of ξ_1 under $\xi_2 = \xi_3 = 0.0$: $\xi_1 = 0.9$ (long dashed lines), 1.0 (solid lines), and 1.1 (short dashed lines).

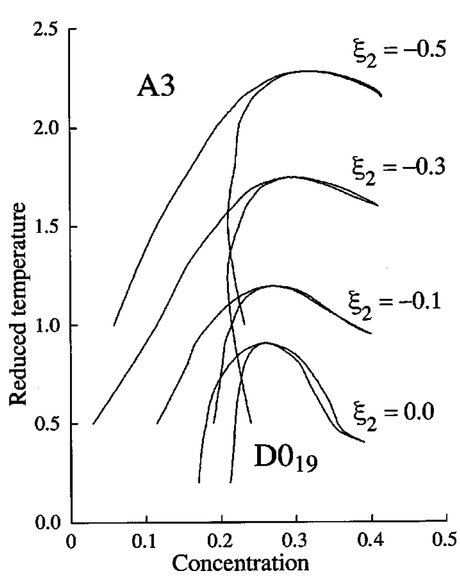

FIG. 4. Changes of the $D0_{19}/A3$ phase boundaries with the variations of ξ_2 from 0.0 to -0.5 under $\xi_1 = 1.0$ and $\xi_3 = 0.0$.

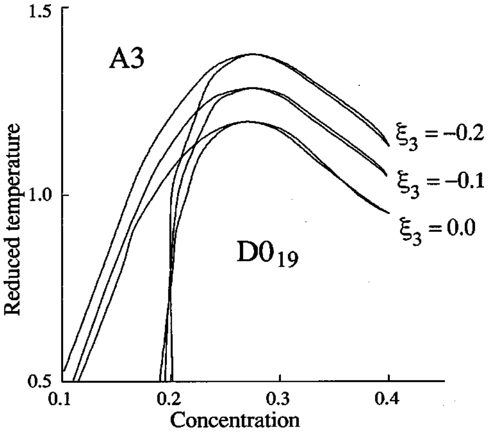

FIG. 5. Changes of the $D0_{19}/A3$ phase boundaries with the variations of ξ_3 from 0.0 to -0.2 under $\xi_1 = 1.0$ and $\xi_2 = -0.1$.

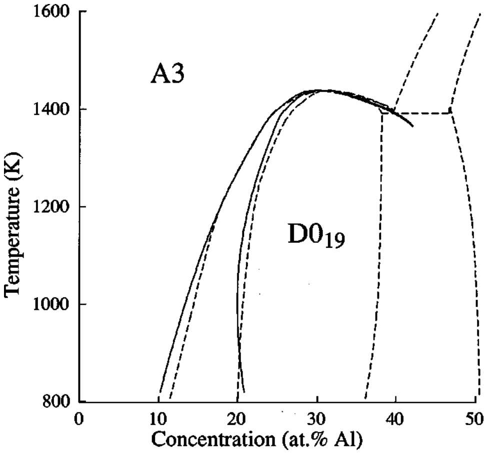

FIG. 6. $D0_{19}/A3$ phase boundaries calculated for $\xi_1 = 1.0$, $\xi_2 = -0.4$, $\xi_3 = -0.1$, and $W_0 = -0.0588$ eV. Dashed lines denote the experimentally determined boundaries (Ref. 27).

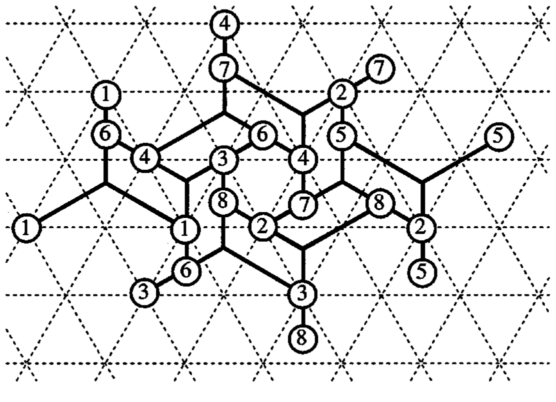

FIG. 7. Top view of the periodic assignment of interpenetrating cells. The circles denote 3×8 sites of the hcp lattice, which are grouped into 8 cells shown by the solid lines.

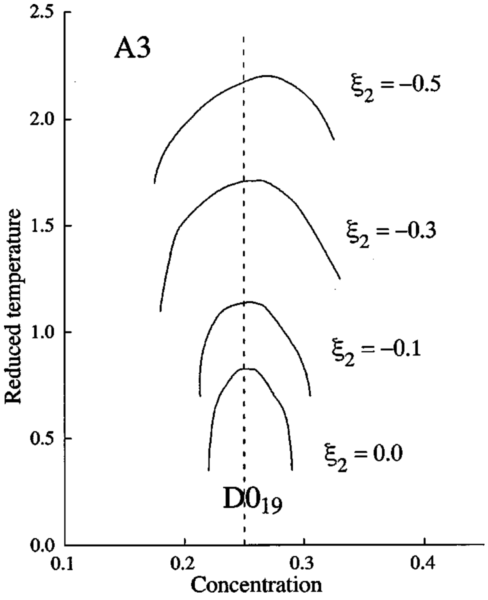

FIG. 8. $D0_{19}/A3$ phase boundaries calculated by the renormalization-group method with the variations of ξ_2 from 0.0 to -0.5 under $\xi_1 = 1.0$ and $\xi_3 = 0.0$. The location of the stoichiometric composition is marked with the dashed line.

remains around the stoichiometric value, which agrees with the earlier study of CVM calculations.[26]

Figure 4 shows the effect of incorporating the second-neighbor interactions. The phase boundaries are drastically changing with decreasing the value of ξ_2 from 0.0 to -0.5. In addition to broadening of the boundary shape, the compositional shift of the congruent point from the stoichiometry to higher values is observed, which is precisely the same feature found in the α/α_2 phase boundaries in the experimental Ti-Al binary phase diagram.[27] If we define the compositional shift δ of the congruent point from the stoichiometric value, the effect of second-neighbor interactions can be estimated as

$$\delta \simeq -0.12\xi_2 + 0.01. \tag{3}$$

Figure 5 shows the effect of the variations of the third-neighbor interactions from $\xi_3 = 0.0$ to -0.2 on the phase boundaries. Besides the trivial shift along the temperature axis, the changes of the shape of the boundaries are rather small in this case.

Although the general contribution from interactions within the third neighbors is the mixture of the above three types of contributions, we can conclude that the essential contribution to the compositional shift of the congruent point of D0$_{19}$/A3 order-disorder transition is that from the second-neighbor interactions, which has been often neglected in the preceding calculations. We have also shown the calculated phase boundaries fitted to the observed α/α_2 phase boundaries[27] in the Ti-Al binary system in Fig. 6. The parameters are chosen to reproduce the observed congruent transition temperature. It suggests that the order of second-neighbor interactions amounts to 40% or more of that of first-neighbor interactions, which is the same order as predicted by the first-principles studies.[15,25]

To ensure the above conclusion, we have also investigated the effect of second-neighbor interactions by using the renormalization-group method. If we define a spin variable σ_p on lattice site p as $+1$ for atom A and -1 for atom B, the Hamiltonian (2) can be written in the following form up to constant terms:

$$H(W_i,\sigma) = -\frac{1}{2}\sum_{\substack{\langle p,q\rangle \\ i\text{th neighbor}}} W_i\sigma_p\sigma_q + \frac{\mu}{2}\sum_p \sigma_p . \tag{4}$$

In the real-space renormalization-group method,[28–31] we divide the original hcp lattice into sublattices or cells and assign a cell-spin σ' to each cell. Then the effective Hamiltonian $H'(W_i',\sigma')$ after the renormalization transformation is calculated from $H(W_i,\sigma)$ by

$$-\beta H'(W_i',\sigma') = \ln\sum_{\sigma} P(\sigma,\sigma')\exp(-\beta H(W_i,\sigma)), \tag{5}$$

where $\beta = 1/kT$ and $P(\sigma,\sigma')$ is the cell-spin weight factor determined by the following way. We first divide the hcp lattice into eight sublattices and define a cell containing three sites in each as illustrated in Fig. 7. Then we assign the cell-spin by using the Niemeijer-van Leeuwen majority rule.[28] This assignment makes the ordered phases (D0$_{19}$ and B19) in question to be transformed into themselves under the renormalization transformation. Thus we have the renormalization-group equations in the following form:

$$W_i' = W_i'(W_0,W_1,W_2). \tag{6}$$

One way to study the phase structure is to investigate the flow of renormalization-group equations (6), and the other way is to evaluate the free energy directly by using the Nauenberg-Niehnuis recursion relation.[29,31] Details of the calculations will be reported elsewhere and the results obtained from the renormalization-group flow are shown in Fig. 8. We can also detect the compositional shift of the congruent point of order-disorder transition and estimate the amount of shift as

$$\delta \simeq -0.06\xi_2 + 0.01. \tag{7}$$

In conclusion, although there is a quantitative difference, both calculations, Monte Carlo simulations and the renormalization-group analyses, suggest that the second-neighbor interactions should play an important role in describing the phase equilibria in hcp binary alloy systems. The situation should be the same in fcc lattices.[1,4,7,14] It is known[5,19] that three-body interactions also make a nontrivial contribution to the shape of phase boundaries and hence the many-body interactions should be included in the future study. However, if we take the interactions beyond the nearest neighbors into account, we can explain the observed shift from stoichiometry of α/α_2 phase boundaries in the Ti-Al binary system within a two-body picture.

The authors are grateful to Professor J. M. Sanchez for his enlightening suggestions on this subject. The numerical calculations were performed on IBM SP-2 and NEC SX-4/20 (Numerical Materials Simulator) at National Research Institute for Metals.

[1] M. K. Phani, J. L. Lebowitz, M. H. Kalos, and C. C. Tsai, Phys. Rev. Lett. **42**, 577 (1979).

[2] K. Binder, Phys. Rev. Lett. **45**, 811 (1980).

[3] K. Binder, J. L. Lebowitz, M. K. Phani, and M. H. Kalos, Acta Metall. **29**, 1655 (1981).

[4] K. Binder, W. Kinzel, and W. Selke, J. Magn. Magn. Mater. **31-34**, 1445 (1985).

[5] D. F. Styer, M. K. Phani, and J. L. Lebowitz, Phys. Rev. B **34**, 3361 (1986).

[6] H. Ackerman, S. Crusius, and G. Inden, Acta Metall. **34**, 2311 (1986).

[7] U. Gahn, J. Phys. Chem. Solids **47**, 1153 (1986).

[8] S. Kämmerer, B. Dünweg, K. Binder, and M. d'Onorio de Meo, Phys. Rev. B **53**, 2345 (1996).

[9] R. Kikuchi, Acta Metall. **25**, 195 (1977).

[10] J. M. Sanchez and D. de Fontaine, Phys. Rev. B **17**, 2926 (1978).

[11] J. M. Sanchez and D. de Fontaine, Phys. Rev. B **21**, 216 (1980).

[12] R. Kikuchi, J. M. Sanchez, H. Yamaguchi, and D. de Fontaine, Acta Metall. **28**, 651 (1980).

[13] C. Sigli and J. M. Sanchez, Acta Metall. **33**, 1097 (1985).

[14] T. Mohri, J. M. Sanchez, and D. de Fontaine, Acta Metall. **33**, 1171 (1985).

[15] M. Asta, D. de Fontaine, M. van Schilfgaarde, M. Sluiter, and M. Methfessel, Phys. Rev. B **46**, 5055 (1992).

[16] F. H. Claro and G. D. Mahan, J. Phys. C **10**, L73 (1977).

[17] G. D. Mahan and F. H. Claro, Phys. Rev. B **16**, 1168 (1977).

[18] M. Schick, J. S. Walker, and M. Wortis, Phys. Rev. B **16**, 2205 (1977).

[19] Z. Ràcz and M. F. Collins, Phys. Rev. B **21**, 229 (1980).

[20] R. Kikuchi, Hughes Research Laboratories Report No. NB80NAAE0188, 1981 (unpublished).

[21] D. Gratias, J. M. Sanchez, and D. de Fontaine, Physica A **113**, 315 (1982).

[22] J. Kanamori, J. Phys. Soc. Jpn. **53**, 250 (1984).

[23] C. Bichara, S. Crusius, and G. Inden, Physica B **179**, 221 (1992).

[24] C. Bichara, S. Crusius, and G. Inden, Physica B **182**, 42 (1992).

[25] M. Asta, D. de Fontaine, and M. van Schilfgaarde, J. Mater. Res. **8**, 2554 (1993).

[26] H. Onodera, T. Abe, and T. Yokokawa, Acta Metall. Mater. **42**, 887 (1994).

[27] J. L. Murray, *Phase Diagrams of Binary Titanium Alloys* (ASM International, Materials Park, OH, 1987).

[28] Th. Niemeijer and J. M. J. van Leeuwen, Phys. Rev. Lett. **31**, 1411 (1973).

[29] M. Nauenberg and B. Nienhuis, Phys. Rev. Lett. **33**, 1598 (1974).

[30] J. M. J. van Leeuwen, Phys. Rev. Lett. **34**, 1056 (1975).

[31] B. Nienhuis and M. Nauenberg, Phys. Rev. B **11**, 4152 (1975).